J Sci Comput (2011) 49:35–50
DOI 10.1007/s10915-010-9445-3

# From Suitable Weak Solutions to Entropy Viscosity

**Jean-Luc Guermond · Richard Pasquetti · Bojan Popov**

Received: 27 January 2010 / Revised: 22 July 2010 / Accepted: 30 November 2010 /
Published online: 16 December 2010


**Abstract** This paper focuses on the notion of suitable weak solutions for the three-dimensional incompressible Navier-Stokes equations and discusses the relevance of this notion to Computational Fluid Dynamics. The purpose of the paper is twofold (i) to recall basic mathematical properties of the three-dimensional incompressible Navier-Stokes equations and to show how they might relate to LES (ii) to introduce an entropy viscosity technique based on the notion of suitable weak solution and to illustrate numerically this concept.

**Keywords** Quality · Reliability · Large-Eddy Simulation, · Suitable weak solutions · Entropy viscosity

## 1 Introduction

The question addressed in this paper is that of constructing approximate solutions to the three-dimensional incompressible Navier-Stokes equations using under-resolved meshes. The use of under-resolved meshes cannot be avoided when the Reynolds number is large, which is very often the case in engineering situations. At the present time, simulating time-dependent flows at Reynolds numbers greater than a few thousands is a challenging task due to the heuristic Kolmogorov estimate $\mathcal{O}(R_e^{9/4})$ for the total number of degrees of freedom which is required to simulate flows at a given value of $R_e$.

In the wake of [9, 12, 13], the objective of this paper is to show that the notion of suitable weak solutions introduced by Scheffer [23] is a sound, firm, mathematical ground which could be useful to LES modelers to build energetically coherent theories.

J.-L. Guermond (✉) · B. Popov
Department of Mathematics, Texas A&M University, College Station, TX 77843, USA
e-mail: guermond@math.tamu.edu

B. Popov
e-mail: popov@math.tamu.edu

R. Pasquetti
Lab. J.A. Dieudonné, UMR CNRS 6621, Université de Nice-Sophia Antipolis, Nice, France
e-mail: Richard.Pasquetti@unice.fr

This paper is organized in four parts. In the first part (Sect. 2) we recall basic mathematical properties of suitable weak solutions and we mention some new results regarding the approximation of these solutions. We want to draw the attention of the community on the fact that, contrary to finite elements/volumes/differences and wavelets, at the time of this writing it is still unknown whether Fourier-based DNS in the periodic cube produce weak solutions that are suitable. In other words there is still no mathematical proof that Fourier-based DNS is energetically consistent. Considering the importance of Fourier-based DNS in CFD, this theoretical gap is worrisome.

In the second part of this paper (Sect. 3) we propose a model that aims at controlling the energy balance at the grid scale in a way which is consistent with the notion of suitable solutions, i.e., suitable solution are locally dissipative. The key idea consists of adding a numerical viscosity proportional to the default to equilibrium in the local energy equation. This model henceforth referred to as LES or entropy viscosity has been proposed in [9, 10].

In the third part (Sect. 4) we test the entropy viscosity technique on some scalar nonlinear conservations laws using various discrete settings comprising Fourier expansions and finite elements.

The entropy viscosity technique is adapted to the compressible Euler equations in the fourth part of this paper (Sect. 5).

The test reported in Sect. 4 and Sect. 5 should convince the reader that computing a numerical viscosity proportional to the entropy residual is a very efficient stabilization technique. We conjecture that this method should be a good candidate for LES and could provide a reasonable mathematical background for LES.

## 2 Suitable Weak Solutions

### 2.1 The Navier-Stokes Problem

Let $\Omega$ be a connected, open, bounded domain in $\mathbb{R}^3$ and consider the time-dependent incompressible Navier-Stokes equations in $\Omega$

$$\begin{cases} \partial_t \mathbf{u} + \mathbf{u}\cdot\nabla\mathbf{u} + \nabla p - R_e^{-1}\Delta\mathbf{u} = \mathbf{f} & \text{in } Q_T, \\ \nabla\cdot\mathbf{u} = 0 & \text{in } Q_T, \\ \mathbf{u}|_{t=0} = \mathbf{u}_0, & \mathbf{u} \text{ periodic or } \mathbf{u}|_\Gamma = 0, \end{cases} \tag{1}$$

where $Q_T = \Omega \times (0, T)$ is the space-time domain, $\Gamma$ is the boundary of $\Omega$, and $R_e$ is the Reynolds number.

Spaces of $\mathbb{R}^3$-valued functions on $\Omega$ and $\mathbb{R}^3$-valued functions are denoted in bold fonts. The Euclidean norm in $\mathbb{R}^3$ is denoted $|\cdot|$. In the following $c$ is a generic constant which may depend on the data $\mathbf{f}$, $\mathbf{u}_0$, $R_e$, $\Omega$, $T$. The value of $c$ may vary at each occurrence. Whenever $E$ is a normed space, $\|\cdot\|_E$ denotes a norm in $E$.

### 2.2 Suitable Weak Solutions

It is known since Leray [19] and Hopf [14] that weak solutions to (1) exist, but the question of uniqueness of these solutions is still open. The major obstacle in the way is that the a priori energy estimates obtained so far do not preclude the occurrence of so-called vorticity bursts reaching scales smaller than the Kolmogorov scale.

Uniqueness is intimately related to smoothness. A very interesting approach to the smoothness question has been developed by Scheffer [23]. The idea is to study the Hausdorff

measure of the singular set of weak solutions (the singular set is composed of those points in time and space where the solution is not essentially bounded in any neighborhood of these points). Proving that the measure of the singular set is zero would amount to proving that there is no singularity. To carry out this program Scheffer introduced the notion of suitable weak solutions which boils down to the following

**Definition 1** Let $(\mathbf{u}, p)$, $\mathbf{u} \in L^2((0,T);\mathbf{H}^1(\Omega)) \cap L^\infty((0,T);\mathbf{L}^2(\Omega))$, $p \in \mathcal{D}'((0,T);L^2(\Omega))$, be a weak solution to the Navier-Stokes equation (1). The pair $(\mathbf{u}, p)$ is said to be suitable if the local energy balance

$$\partial_t\left(\frac{1}{2}\mathbf{u}^2\right) + \nabla\cdot\left(\left(\frac{1}{2}\mathbf{u}^2 + p\right)\mathbf{u}\right) - R_e^{-1}\Delta\left(\frac{1}{2}\mathbf{u}^2\right) + R_e^{-1}(\nabla\mathbf{u})^2 - \mathbf{f}\cdot\mathbf{u} \leq 0 \tag{2}$$

is satisfied in the distributional sense, i.e., in $\mathcal{D}'(Q_T;\mathbb{R}^+)$.

It is remarkable that the above inequality is similar to entropy conditions for conservation laws. Think of it as an entropy inequality where the kinetic energy would play the role of an entropy.

Suitable weak solutions are known to exist always. They can be constructed by regularizing the nonlinear term (i.e., Leray regularization) and passing to the limit. With this notion Scheffer was able to derive a bound from above of some Hausdorff measure of the singular set. The remarkable fact about this result is that it cannot (yet) be obtained without invoking suitability, i.e., it is not known if every weak solution satisfies (2). The result of Scheffer has been improved by Caffarelli-Kohn-Nirenberg and is now referred as the Caffarelli-Kohn-Nirenberg Theorem [4, 21] in the literature. In a nutshell, this result asserts that the one-dimensional Hausdorff measure of the set of singularities of a suitable weak solution is zero. In other words, if singularities exist, they must lie, on a space-time set whose dimension is smaller than that of a space-time line. To the present time, this is the best partial regularity result available for the Navier-Stokes equations. For any practical purpose, this theorem asserts that suitable weak solutions are almost classical. The word "almost" is important here; although suitable weak solutions are the most regular solutions known to exist, they may still have singular points, i.e., be not classical.

### 2.3 Direct Numerical Simulations (DNS)

Since DNS is the highest court in LES-land, one is certainly entitled to ask whether limits of DNS solutions (as the mesh-size goes to zero) are suitable. This may seem to be a dumb question to ask, but surprisingly the answer is not yet totally clear.

To formalize an answer to the above question let us assume that the velocity and pressure are approximated in some discrete spaces $\mathbf{X}_h$ and $M_h$, respectively ($h$ denoting the mesh-size). We now introduce a notion of discrete commutator.

**Definition 2** The space $\mathbf{X}_h$ (resp. $M_h$) is said to have the discrete commutator property if there is an operator $P_h \in \mathcal{L}(\mathbf{H}_0^1(\Omega);\mathbf{X}_h)$ (resp. $Q_h \in \mathcal{L}(H^1(\Omega);M_h)$) such that the following holds for all $\phi$ in $W_0^{2,\infty}(\Omega)$ and all $v_h \in \mathbf{X}_h$ (resp. all $q_h \in M_h$)

$$\|\phi v_h - P_h(\phi v_h)\|_{\mathbf{H}^l(\Omega)} \leq c\,h^{1+m-l}\|v_h\|_{\mathbf{H}^m(\Omega)}\|\phi\|_{W^{m+1,\infty}(\Omega)}, \qquad 0 \leq l \leq m \leq 1,$$

$$\|\phi q_h - Q_h(\phi q_h)\|_{H^l(\Omega)} \leq c\,h^{1+m-l}\|q_h\|_{H^m(\Omega)}\|\phi\|_{W^{m+1,\infty}(\Omega)}.$$

When $P_h$ (resp. $Q_h$) is a projector, the above definition is an estimate of the operator norm of the commutator $[\Phi, P_h] := \Phi \circ P_h - P_h \circ \Phi$ where $\Phi(v) := \phi v$. This property is also called 'super-approximation' in the finite element literature [13, 15, 16]. The discrete commutator property is known to hold in discrete spaces where there exist projectors that have local approximation properties, see Bertoluzza [3]. It is known to hold for finite elements and wavelets.

The best available results so far concerning the construction of suitable weak solution as limits of DNS solution is summarized in the following

**Theorem 1** (See [7, 8]) *If* $\mathbf{X}_h$ *and* $M_h$ *have the discrete commutator property* (*in addition to having the usual reasonable approximation properties*), *the pair* $(u_h, p_h)$ *convergences*, *up to subsequences*, *to a suitable weak solution to* (1).

In a nutshell this theorem says that DNS solutions based on finite elements and wavelets (and very likely finite volumes and finite differences, splines, etc.) converge to suitable weak solutions.

One may then wonder if DNS solutions based on Fourier approximation in the periodic cube also converge to suitable solutions. Surprisingly enough, this is still unknown at the time of this writing. The main obstacle in the way is that the discrete commutator property does not hold for Fourier approximations. Actually, counter-examples to the discrete commutator property can be constructed. We are then led to seriously consider the following

**Open question 1** Do Fourier-based DNS solutions converge to suitable weak solution as the degree of the approximation goes to infinity?

We think this question should equally attract the interest of mathematicians and DNS specialists. For mathematicians, investigating this problem might be a way to set a wedge that could separate the class of suitable weak solutions from that of those that are weak only. For CFD specialists, it would certainly be re-assuring to know that Fourier-based DNS solutions locally dissipate energy correctly.

One way to interpret the above results is that Finite Elements, Wavelets, Finite Differences, etc. have enough built-in numerical dissipation to help the energy cascade to go in the right direction, i.e., the energy at extremely fine scales is always dissipated when using approximation methods having local interpolation properties. Contrary to Finite Elements, wavelets, etc. the Fourier technique is so accurate that it does not induce enough numerical diffusion to counteract the Gibbs-Wilbraham phenomenon. Whether energy is correctly dissipated locally for Fourier approximations is still a mystery. The key here is the lack of localization of the Fourier approximation.

### 2.4 More Open Questions for DNS

Let us finish this section by bringing the following open question to the attention of the DNS community

**Open question 2** Do weak solutions to the Navier-Stokes equation satisfy the global energy balance?

Again, this question may seem ridiculous, but global energy balance has not yet been proved for large data (initial or forcing term). The DNS community could contribute to

solving this question by verifying the global energy balance of DNS solutions as the mesh size is refined.

Of course, calling $\mathbf{u}_h$ the DNS solution, it is clear that any DNS algorithm can be tweaked so that global energy balance is exact

$$\frac{1}{2}\|\mathbf{u}_h(T)\|^2_{\mathbf{L}^2(\Omega)} + \int_0^T R_e^{-1}\|\nabla\mathbf{u}_h(t)\|_{\mathbf{L}^2(\Omega)}\,\mathrm{d}t = \frac{1}{2}\|\mathbf{u}_0\|^2_{\mathbf{L}^2(\Omega)}. \tag{3}$$

This is not the point. Unless it can be proved someday that $\mathbf{u}_h$ converges strongly to some $\mathbf{u}$ in $L^2((0,T);\mathbf{H}^1(\Omega))$, there is no reason for the limit solution, say $\mathbf{u}$, to satisfy the equality in (3). The best that can be deduced from the uniform boundedness of $\mathbf{u}_h$ in $L^2((0,T);\mathbf{H}^1(\Omega))$ is the inequality

$$\frac{1}{2}\|\mathbf{u}(T)\|^2_{\mathbf{L}^2(\Omega)} + \int_0^T R_e^{-1}\|\nabla\mathbf{u}(t)\|_{\mathbf{L}^2(\Omega)}\,\mathrm{d}t \le \frac{1}{2}\|\mathbf{u}_0\|^2_{\mathbf{L}^2(\Omega)}. \tag{4}$$

More precisely, although $\nabla\mathbf{u}_h$ converges weakly to $\nabla\mathbf{u}$ in $\mathbf{L}^2(Q_T)$, it is possible that $\lim_{h\to 0}\|\nabla\mathbf{u}_h\|_{\mathbf{L}^2(\Omega)} \not\to \|\nabla\mathbf{u}\|_{\mathbf{L}^2(Q_T)}$. To understand the difficulty, assume that $1/h \in \mathbb{N}$ and consider of the function

$$v_h(x) = \sin(2\pi x/h), \quad x \in (0,1). \tag{5}$$

Clearly $v_h \to 0$ weakly in $L^2(0,1)$ as $h \to 0$, but $\|v_h\|_{L^2(0,1)} = \frac{1}{2}$ and $\|\lim_{h\to 0} v_h\|_{L^2(0,1)} = 0$. In other words $\lim_{h\to 0}\|v_h\|_{L^2(0,1)} \neq \|\lim_{h\to 0} v_h\|_{L^2(0,1)}$. It is remarkable though that any amount of smoothing is sufficient to transform weak convergence into strong convergence. Hence, extending $v_h$ by zero over $\mathbb{R}$ it can be shown that $\lim_{h\to 0}\|\varphi_\epsilon * v_h\|_{L^2(0,1)} = \|\lim_{h\to 0}\varphi_\epsilon * v_h\|_{L^2(0,1)}$ for any reasonable smoothing kernel $\varphi$ and any $\epsilon > 0$.

Upon setting $\overline{\mathbf{u}}_h(t) := \varphi_\epsilon * \mathbf{u}_h(t)$, DNS simulations could help solve the above question by verifying whether the following holds for all times $T$

$$\frac{1}{2}\|\overline{\mathbf{u}}_h(T)\|^2_{\mathbf{L}^2(\Omega)} + \int_0^T R_e^{-1}\|\nabla\overline{\mathbf{u}}_h(t)\|_{\mathbf{L}^2(\Omega)}\,\mathrm{d}t \approx \frac{1}{2}\|\mathbf{u}_0\|^2_{\mathbf{L}^2(\Omega)} \tag{6}$$

for small resolutions (i.e., $h \to 0$) and any $\epsilon \gg h$, say $\epsilon = h^\alpha$ with $\alpha \in (0,1)$.

## 3 Proposal for a LES Model Based on Suitability

The goal of this section is to explore some implications the notion of suitable solutions may have when it comes to approximate the Navier-Stokes equations on a finite grid. In other words, since $\lim_{h\to 0}$ is a mathematical dream which is unachievable with the computing power currently available, can we anyway draw something useful from the existence of suitable solutions?

### 3.1 Practical Interpretation of the Notion of Suitable Solution

At high Reynolds numbers CFD is always under-resolved. In other words, even if one uses a discrete setting admitting a discrete commutator property, the results of Theorem 1 is useless for practical purposes since the approximate solution thus calculated may be far from a (the?) suitable solution. The limit $h \to 0$ is an ideal situation from which practical

CFD simulations are usually far. Then, one may ask oneself what is the use of the notion of suitable solutions? Is it a notion that we should care about in CFD?

To answer the above question, let us rephrase the definition of suitability. Let $\mathbf{u}$, $p$ be a weak solution of the Navier-Stokes equations in the Leray class. Let us define the residual of the momentum equation

$$\mathbf{R}(\mathbf{x},t) := \partial_t \mathbf{u} - R_e^{-1}\Delta\mathbf{u} + \mathbf{u}\cdot\nabla\mathbf{u} + \nabla p - \mathbf{f}. \tag{7}$$

$\mathbf{u}$, $p$ being a weak solution means that the residual $\mathbf{R}(\mathbf{x},t)$ is zero in the distribution sense. Is it then clear that the power of the residual, $\mathbf{R}(\mathbf{x},t)\cdot\mathbf{u}$, is zero? Well, no, since it is not known whether $\mathbf{u}$ is smooth enough for the product $\mathbf{R}(\mathbf{x},t)\cdot\mathbf{u}(\mathbf{x},t)$ to be an integrable function, i.e., it is not clear whether the integral $\int_0^T \int_\Omega \mathbf{R}(\mathbf{x},t)\cdot\mathbf{u}(\mathbf{x},t)\,\mathrm{d}\mathbf{x}\,\mathrm{d}t$ makes sense.

Consider the one-dimensional inviscid Burgers equation $\partial_t u + \frac{1}{2}\partial_x(u^2) = 0$ for instance. In the distribution sense $0 = R(x,t) := \partial_t u + \frac{1}{2}\partial_x(u^2)$, but the unique entropy solution is, among all the weak solutions, the only one that satisfies $R(x,t)u = \frac{1}{2}\partial_t u^2 + \frac{1}{3}\partial_x(u^3) \le 0$. It is indeed true that the product $R(x,t)u = 0$ at points $(x,t)$ where $u$ is smooth, but in shocks $R(x,t)u$ is a negative Dirac measure. More precisely consider the following solution $u(x,t) = 1 - H(x - \frac{1}{2}t)$ where $H$ is the Heaviside function, $x \in (-\infty, +\infty)$ and $t \ge 0$. One easily verifies that $u$ solves the Burgers equations with initial data $u_0(x) = 1 - H(x)$, i.e., $R(x,t) = 0$, but $\frac{1}{2}\partial_t u^2 + \frac{1}{3}\partial_x(u^3) = -\frac{1}{12}\delta(x - \frac{1}{2}t) \neq 0$, where $\delta$ is the Dirac measure. This example may help the reader to understand why the Open question 2 is still open and might not have an obvious answer. When approximating the solutions of the Burgers equation, one can certainly come up with algorithms that are energy preserving (i.e., $\int_{-\infty}^{\infty} \frac{1}{2}u_h^2(x,t)\,\mathrm{d}x = \int_{-\infty}^{\infty} \frac{1}{2}u_0^2(x)\,\mathrm{d}x$). Using such a technique would be a disastrous idea, since the energy preserving solution to the Burgers equation is not the correct one.

The definition of a suitable solution can be rephrased as follows: a suitable solution is one for which the power of the residual is negative in the distribution sense in $Q_T$, i.e.,

$$\partial_t(\tfrac{1}{2}\mathbf{u}^2) + \nabla\cdot((\tfrac{1}{2}\mathbf{u}^2 + p)\mathbf{u}) - R_e^{-1}\Delta(\tfrac{1}{2}\mathbf{u}^2) + R_e^{-1}(\nabla\mathbf{u})^2 - \mathbf{f}\cdot\mathbf{u} \le 0. \tag{8}$$

The reader may verify by himself that indeed, (8) is formally equivalent to $\mathbf{R}(\mathbf{x},t)\cdot\mathbf{u} \le 0$, (the term "formally" meaning: in the optimistic hypothesis that $\mathbf{u}$ and $p$ are smooth functions). In other words, if singularities occur, suitable solutions are such that these singularities dissipate energy.

### 3.2 What Happens in Under-Resolved Simulations?

Let us now focus our attention on under-resolved numerical simulations. Being under-resolved in a space-time region means that the numerical solution experiences large gradients that cannot be correctly represented by the mesh in the region in question. In other words, for all practical purpose, the numerical solution is singular at the considered mesh scale (i.e., behaves like a singular one on the available mesh). As time progresses the large unresolved gradients are likely to produce even larger gradients through nonlinear interactions, i.e., we have to deal with energy accumulation at the grid scale. The question is no longer to determine whether the solution(s) to the Navier-Stokes equation is (are) classical or not (a debate that a pragmatic reader may think to be of remote academic interest), it just now amounts to deciding what to do with a quasi-singular numerical solution.

Let us rephrase the situation in mathematical terms. Let $(\mathbf{u}_h, p_h)$ be the approximate velocity and the approximate pressure, the subscript $h$ representing the typical mesh-size.

Let $D_h(\mathbf{x},t)$ be the numerical residual of the energy (entropy) equation

$$D_h(\mathbf{x},t) := \partial_t\left(\frac{1}{2}\mathbf{u}_h^2\right)+\nabla\cdot\left(\left(\frac{1}{2}\mathbf{u}_h^2+p_h\right)\mathbf{u}_h\right)-R_e^{-1}\Delta\left(\frac{1}{2}\mathbf{u}_h^2\right)+R_e^{-1}(\nabla\mathbf{u}_h)^2-\mathbf{f}\cdot\mathbf{u}_h. \quad (9)$$

Being under-resolved in a neighborhood of $(x_0,t_0)$ means that $D_h(x_0,t_0)$ is significantly larger than the consistency error of the method. If locally the power of the numerical singularity is negative, i.e., $D_h(x_0,t_0)\le 0$, we do not have anything to fear since energy is cascading down and is eventually lost in the subgrid scales, a scenario in agreement with the Kolmogorov cascade. On the other hand if the numerical singularity produces energy, i.e., $D_h(x_0,t_0)>0$, all the bets are off since the situation is out of control and, by analogy with a shock that would produce energy, is unphysical.

In conclusion ensuring that $D_h(x_0,t_0)\le 0$ is a highly desirable feature. If it could be enforced everywhere in the domain, that would mean that the energy gently cascades down in the subgrid scales and is eventually dissipated. Rephrased in eddy terms, this condition would guaranty that every eddy of size similar to the mesh-size would eventually be dissipated. Hence in under-resolved situations, one should wish the approximate solution to be suitable in the discrete sense, i.e.,

$$D_h(\mathbf{x},t)\le\epsilon(h),\quad \forall(\mathbf{x},t)\in Q_T, \quad (10)$$

with $\epsilon(h)\ge 0$ and $\lim_{h\to 0}\epsilon(h)=0$.

### 3.3 A LES Model Based on Suitability

Of course (10) cannot be enforced in addition to the discrete momentum conservation and the discrete mass conservation. But, similarly to the entropy condition for nonlinear conservation laws, (10) can be incorporated in the algorithm that calculates the pair $(\mathbf{u}_h, p_h)$.

Possibilities are numerous, but the technique that we propose is to use (10) to construct an artificial viscosity by setting

$$\nu_h(\mathbf{x},t) := \min\left(c_{\max}|\mathbf{u}_h(\mathbf{x},t)|h(x), c\,h^2(x)\frac{|D_h(\mathbf{x},t)|}{\|\mathbf{u}_h^2\|_{\mathbf{L}^\infty(\Omega)}}\right), \quad (11)$$

where $h(x)$ is the local mesh size in the neighborhood of $x$, $\|\mathbf{u}_h^2\|_{\mathbf{L}^\infty(\Omega)}$ is the maximum norm of $\mathbf{u}_h^2$ (this is just a normalizing term), $c_{\max}\approx 0.5$ and $c$ are adjustable constants. When normalization is done properly we have found $c\approx 0.25$ to be appropriate. The momentum equation is then modified by adding the term $-\nabla\cdot(\nu_h(\mathbf{x},t)\nabla\mathbf{u}_h)$. Since $\frac{1}{2}|\mathbf{u}_h(\mathbf{x},t)|h(x)$ is the viscosity that is induced by first-order up-winding on a uniform Cartesian grid, using $c_{\max}=\frac{1}{2}$ in the above formula roughly amount to limit the viscosity with the first-order upwind viscosity on uniform Cartesian grids. Definition (11) implies that the LES viscosity never exceeds the first-order up-wind viscosity. When the mesh is fine enough to resolve all the scales, the quantity $|D_h(\mathbf{x},t)|$ is of the same order as the consistency error of the numerical method which is used and $h(x)^2|D_h(\mathbf{x},t)|$ is far smaller than the first-order upwind viscosity. This observation implies that $\nu_h(\mathbf{x},t)$ is a consistent viscosity, i.e., it vanishes when all the scales are resolved. The LES viscosity is active only in under-resolved region if spurious energy is generated at the mesh scale, i.e., when energy seems to be coming up from subgrid scales. Note that the LES viscosity as defined in (11) may be oscillatory, so that smoothing of $\nu_h$ (local averaging) may be required.

Let us finish by mentioning that the choice that we made of enforcing (10) by using a dissipative model is not unique. We conjecture that it might also be possible to mimic (10) by using other techniques like filtering and approximate deconvolution which are more popular in the LES community [1].

## 4 Numerical Illustrations for Scalar Conservation Laws

Our goal in this section is to describe how the LES viscosity model proposed above can be used to solve nonlinear scalar conservations laws. We change the terminology by renaming the LES viscosity an entropy viscosity.

### 4.1 Scalar Conservation Equations

We consider the equation

$$\partial_t u + \nabla\cdot\mathbf{f}(u) = 0 \tag{12}$$

subject to the initial condition $u|_{t=0} = u_0$ and the appropriate boundary conditions. In some cases we will solve the Cauchy problem (restricted to a bounded domain) and in other cases we will specify the corresponding boundary conditions. It is well known that the Cauchy or the initial boundary value problem has a unique entropy solution (see [2, 17]) which satisfies an additional set of differential inequalities

$$\partial_t E(u) + \nabla\cdot\mathbf{F}(u) \le 0 \tag{13}$$

for any pair of functions $E(u)$ and $\mathbf{F}(u)$ such that $E$ is convex and $\mathbf{F}(u) = \int E'(u)\mathbf{f}'(u)\,\mathrm{d}u$. The function $E$ is called entropy and $\mathbf{F}$ is the associated entropy flux. The most well known pairs are the Kružkov's pairs generated by $E_c(u) = |u-c|$, where $c$ is any arbitrary constant. It is known that $E(u) = \frac{1}{2}u^2$ is enough to select the unique entropy solution when $\mathbf{f}$ is convex.

### 4.2 The Algorithm

Assume that we have at hand a finite element mesh $\mathcal{T}_h$ and that the local approximation is done using polynomials of degree at most $k$. We first assume that the time is continuous. The entropy viscosity method proceeds as follows:

- Compute the entropy residual, $D_h(u) := \partial_t E(u) + \nabla\cdot\mathbf{F}(u)$.
- For each cell $K \in \mathcal{T}_h$ compute the local mesh size: $h_K = \mathrm{diam}(K)/k$.
- Let $\overline{E}(u_h)$ be the average entropy over the domain. On each cell, construct a viscosity associated with the entropy residual:

$$\nu_E := c_E\, h_K^2 \|D_h\|_{L^\infty(K)} / \|E(u_h) - \overline{E}(u_h)\|_{L^\infty(\Omega)}.$$

- On each cell, compute an upper bound of the viscosity based on the maximum local wave speed: $\beta_K = \||\mathbf{f}'(u)|\|_{\infty,K}$, where $|\cdot|$ is the Euclidean norm:

$$\nu_{\max} := c_{\max} h_K \beta_K.$$

- Define the entropy viscosity on each mesh cell $K$:

$$\nu_h := \min(\nu_{\max}, \nu_E). \tag{14}$$

  If required, one may smooth the thus obtained entropy viscosity. This is especially useful when high order approximations are concerned, i.e. if $k > 2$ (see the companion paper [11]).
- Solution method: Galerkin + entropy viscosity:

$$\int_\Omega (\partial_t u_h + \nabla\cdot\mathbf{f}(u_h) v_h \,\mathrm{d}\mathbf{x} + \sum_K \int_K \nu_h \nabla u_h \cdot \nabla v_h \,\mathrm{d}\mathbf{x} = 0, \quad \forall v_h.$$

The time marching can be done with an explicit Runge-Kutta method (RK3 or RK4). Denoting $u_h^n$, $u_h^{n-1}$ and $u_h^{n-2}$, the approximations of $u$ at time $t_n$, $t_{n-1}$ and $t_{n-2}$, one simple possibility to evaluate the entropy residual consists of setting

$$D_h = \frac{1}{2\Delta t}(3E(u_h^n) - 4E(u_h^{n-1}) + E(u_h^{n-2})) + \nabla\cdot\mathbf{F}(u_h^n), \tag{15}$$

which is formally second-order accurate in time.

### 4.3 Inviscid Burgers Equation

To numerically illustrate the above algorithm we first consider the inviscid Burgers equation in two space dimensions with $\mathbf{f}(u) = \frac{1}{2}(u^2, u^2)$ and $E(u) = \frac{1}{2}u^2$. The initial data is piecewise constant in the four quadrants of $\mathbb{R}^2 + (\frac{1}{2}, \frac{1}{2})$; $u_0 = -1, -0.2, 0.5, 0.8$ in the top right, top left, bottom left, and bottom right quadrant, respectively. The field $u_0$ is shown in the left panel of Fig. 1. The solution computed with $\mathbb{P}_1$ elements ($3\,10^4$ $\mathbb{P}_1$ nodes) is shown in the right panel of Fig. 1.

We perform convergence tests in the square $(0, 1)^2$. The tests are done with $\mathbb{P}_1$ and $\mathbb{P}_2$ Lagrange finite elements on unstructured Delaunay meshes. The solution is computed at $t = 0.5$ and the error is measured in the $L^1$- and $L^2$-norm. We report in Table 1 the results obtained with $\mathbb{P}_1$ and $\mathbb{P}_2$ Lagrange finite elements on various meshes. The quantity $h$

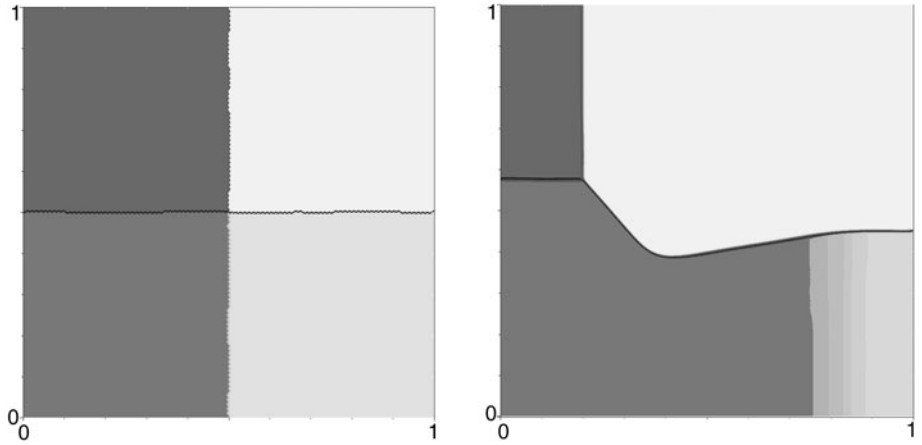


**Fig. 1** Burgers. Initial data (*left*); $\mathbb{P}_1$ approximation at $t = 0.5$, $3\,10^4$ nodes (*right*)

**Table 1** Convergence tests for the inviscid Burgers equation. $\mathbb{P}_1$ approximation (*left*), $\mathbb{P}_2$ approximation (*right*)

| $h$ | $\mathbb{P}_1$ | | | | $\mathbb{P}_2$ | | | |
|---|---|---|---|---|---|---|---|---|
| | $L^2$ | Rate | $L^1$ | Rate | $L^2$ | Rate | $L^1$ | Rate |
| 5.00E–2 | 2.3651E–1 | – | 9.3661E–2 | – | 1.8068E–1 | – | 5.2531E–2 | – |
| 2.50E–2 | 1.7653E–1 | 0.422 | 4.9934E–2 | 0.907 | 1.2956E–1 | 0.480 | 2.7212E–2 | 0.949 |
| 1.25E–2 | 1.2788E–1 | 0.465 | 2.5990E–2 | 0.942 | 9.5508E–2 | 0.440 | 1.4588E–2 | 0.899 |
| 6.25E–3 | 9.3631E–2 | 0.449 | 1.3583E–2 | 0.936 | 6.8806E–2 | 0.473 | 7.6435E–3 | 0.932 |
| 3.12E–3 | 6.7498E–2 | 0.472 | 6.9797E–3 | 0.961 | – | – | – | – |

**Table 2** Convergence tests for Burgers. Fourier approximation

| $N$ | $h = 1/N$ | $L^1$ | Rate | $L^2$ | Rate |
|---|---|---|---|---|---|
| 36 | 2.78E–2 | 1.92E–2 | – | 1.02E–1 | – |
| 72 | 1.39E–2 | 9.99E–3 | 0.94 | 7.28E–2 | 0.49 |
| 144 | 6.94E–3 | 5.34E–3 | 0.89 | 5.41E–2 | 0.43 |
| 288 | 3.47E–3 | 2.79E–3 | 0.95 | 3.80E–2 | 0.51 |

refers to the typical mesh-size for each mesh. The time stepping is done using the SSP RK3 method, see [6]. The entropy residual is computed with the explicit BDF2 formula (15) based on the three previous time levels. The coefficients $c_{\max}$ and $c$ in (14) are $c_{\max} = 0.4/k$ and $c_E = 1$. As expected, the convergence rates in the $L^1$- and $L^2$-norms are close to the theoretical $\mathcal{O}(h)$ and $\mathcal{O}(h^{\frac{1}{2}})$ orders, respectively. The $\mathcal{O}(h)$ order is optimal since the total variation with respect to space of the solution is bounded for all time but the gradient is not integrable, i.e., $u(\cdot, t) \in BV$ but $u(\cdot, t) \notin W^{1,1}$. A similar remark holds for the $\mathcal{O}(h^{\frac{1}{2}})$ convergence order in the $L^2$-norm.

We now redo the above convergence tests with Fourier expansions, see [11] for details on the algorithm. The results are reported in Table 2. The computation is done by extending the computational domain by symmetry about the axes $\{x = 1\}$ and $\{y = 1\}$ and the initial data is extended so as to make the extension periodic. The time marching is done by using the standard Runge-Kutta scheme (RK4). The nonlinearity is de-aliased using the $\frac{3}{2}$-padding rule. The entropy viscosity is made explicit and computed by using the BDF2 formula (15) based on the three previous time levels. The entropy viscosity is computed in the physical space at the Fourier nodes. The coefficients $c_{\max}$ and $c$ in (14) are $c_{\max} = 0.5$ and $c_E = 8$. Here again we observe quasi-optimal convergence rates both in $L^1$- and $L^2$-norms.

### 4.4 KPP Rotating Wave

We now illustrate the capability of the entropy viscosity method to deal with non-convex fluxes by solving the two-dimensional scalar conservation law

$$\partial_t u + \nabla \cdot \mathbf{f}(u) = 0, \quad \mathbf{f}(u) = (\sin u, \cos u) \tag{16}$$

subject to the following initial condition

$$u(x, y, 0) = u_0(x, y) = \begin{cases} 3.5\pi, & x^2 + y^2 < 1; \\ 0.25\pi, & \text{otherwise.} \end{cases} \tag{17}$$

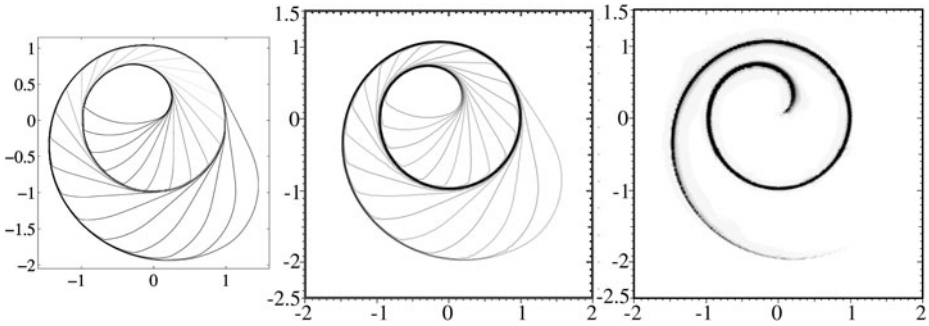

**Fig. 2** KPP rotating wave. *Left*: Adaptive WENO5/Minmod 1 from [18] on Cartesian grid $\Delta x = \Delta y = \frac{1}{100}$; *Center*: entropy-viscosity $\mathbb{P}_2$ approximation, $h = 0.0125$; *Right*: Ratio of the entropy viscosity to its maximum value

This test proposed in [18] is a challenging exercise to many high-order numerical schemes because the exact solution has a two-dimensional composite wave structure. For example the central-upwind schemes based on WENO5, Minmod 2 and SuperBee reconstructions fail this test case, see [18] for details.

The solution is computed at $t = 1.0$ and is shown in Fig. 2. The left panel shows the reference solution from [18] on a Cartesian grid $400 \times 400$, i.e., $h = 0.01$. This solution is computed using an adaptive WENO5/Minmod 1 reconstruction; the Minmod 1 reconstruction is used only in the transition zones where the flux convexity changes and WENO5 is used everywhere else. The center panel shows the $\mathbb{P}_2$ approximation using the entropy viscosity on a quasi-uniform mesh of mesh size $h = 0.0125$. The composite wave is captured well and the accuracy of the $\mathbb{P}_2$ approximation is similar to that of the reference solution. The right panel shows the ratio of the entropy viscosity to the first-order upwind viscosity, which is very small outside the shock and saturates to 1 in the shock, as expected. This panel illustrates quite well the auto-adaption property of the entropy viscosity.

## 5 Numerical Illustration for the Euler Equations

We extend in this section the entropy viscosity method to the compressible gas dynamics for perfect gases.

### 5.1 The Euler Equations

We consider the Euler equations for a perfect gas. These equations state the conservation of mass, momentum and energy (see, e.g., [20] for an overview) and can be put into the following conservative form:

$$\partial_t \mathbf{c} + \nabla\cdot(\mathbf{f}(\mathbf{c})) = 0, \quad \mathbf{c} = \begin{pmatrix} \rho \\ \mathbf{m} \\ E \end{pmatrix}, \quad \mathbf{f}(\mathbf{c}) = \begin{pmatrix} \mathbf{m} \\ \mathbf{m} \otimes \frac{\mathbf{m}}{\rho} + p\mathbb{I} \\ \frac{\mathbf{m}}{\rho}(E + p) \end{pmatrix}, \tag{18}$$

where the independent variables are the density $\rho$, the momentum vector field $\mathbf{m}$ and the total energy $E$. The velocity vector field $\mathbf{u}$ is defined by $\mathbf{u} := \mathbf{m}/\rho$. The symbol $\mathbb{I}$ denotes the identity matrix in $\mathbb{R}^d$. The pressure is expressed via the equation of state of ideal gases:

$$p = \rho T, \quad \text{with } T = (\gamma - 1)\left(\frac{E}{\rho} - \frac{1}{2}\mathbf{u}^2\right), \tag{19}$$

where $\gamma$ is the adiabatic constant and $T$ is the temperature. We also introduce the entropy functional

$$S(p,\rho)=\frac{\rho}{\gamma-1}\log(p/\rho^{\gamma}). \tag{20}$$

This quantity satisfies the following inequality

$$\partial_t S+\nabla\cdot(\mathbf{u}S)\geq 0, \tag{21}$$

with equality if all the fields are smooth.

### 5.2 Description of the Algorithm for Finite Elements

The main idea of the algorithm consists of introducing an artificial viscosity and an artificial thermal diffusivity in the spirit of the compressible Navier-Stokes equations, i.e., we augment the Euler system with additional viscous fluxes. This idea has been investigated in [10] in one space dimension using Fourier expansions for space approximation. The algorithm that we presently use is slightly simplified.

This algorithm proceeds similarly to what is described in Sect. 4.2 for scalar conservation laws. At each time step we do the following: (i) we evaluate the residual of the entropy equation, (ii) we compute the associated artificial viscosities, (iii) then we update the mass, momentum, and total energy, the fluxes being augmented with the following viscous flux

$$\mathbf{f}_{visc}(\mathbf{c}_h)=\begin{pmatrix}0\\ -\mu_h\nabla\mathbf{u}_h\\ -\mu_h\nabla(\frac{1}{2}\mathbf{u}_h^2)-\kappa_h\nabla T_h\end{pmatrix}. \tag{22}$$

Let us now be more specific. Let $\Delta t$ be the time step and let $\mathbf{c}_h^n$, $\mathbf{c}_h^{n-1}$, etc. be the approximations of the solution at times $t_n$, $t_{n-1}$, etc. We define the physical entropy $S_h^n=\frac{\rho_h^n}{\gamma-1}\log(p_h^n/(\rho_h^n)^{\gamma})$. Then the task consists of evaluating the residual for the entropy conservation equation. One possible option consists of setting,

$$D_h=\tfrac{1}{2\Delta t}(3S_h^n-4S_h^{n-1}+S_h^{n-2})+\nabla\cdot(\mathbf{u}_h^n S_h^n), \tag{23}$$

which is formally second-order accurate. For each mesh cell $K$ in $\mathcal{T}_h$ we then compute the entropy viscosity associated with the residual:

$$\mu_S=c_E h_K^2\|\rho_h\|_{L^\infty(K)}\|D_h\|_{L^\infty(K)}. \tag{24}$$

Note that $\mu_S$ has the right dimension and that no normalization is needed, since the log coming in the definition of the physical entropy is dimensionless.

Since $((\mathbf{u}_h^n)^2+\gamma T_h^n)^{\frac{1}{2}}$ is an upper bound on all the local wave speeds, we estimate the first-order upwind viscosity as follows:

$$\mu_{\max}=c_{\max}h_K\|\rho_h^n((\mathbf{u}_h^n)^2+\gamma T_h^n)^{\frac{1}{2}}\|_{L^\infty(K)}. \tag{25}$$

Taking $c_{\max}=\frac{1}{2}$ would roughly amount to limit the viscosity with the first-order upwind viscosity on uniform Cartesian grids.

Finally, we set:

$$\mu_h=\min(\mu_{\max},\mu_S), \tag{26}$$

$$\kappa_h=\mathcal{P}\frac{\mu_h}{\gamma-1}. \tag{27}$$

In the previous expressions the tunable coefficients $c_{\max}$ and $c_E$ depend on the time-marching technique and on the space approximation method, but are independent of the time step $\Delta t$ and the mesh-size $h$. The coefficient $\mathcal{P}$ is an artificial Prandtl number which can be chosen to be of order 1.

This approach gives satisfactory results, but we sometimes observe small spurious oscillations of the density field. One way to improve the situation is to add an artificial diffusion term on the density. Improvements can indeed be obtained by augmenting the continuity equation with a dissipation term, which viscosity, say $\nu_h$, is again linked to $\mu_h$ as follows $\nu_h = \mathcal{P}_\rho \mu_h / \|\rho_h\|_{L^\infty(K)}$. In practice using $\mathcal{P}_\rho \in [0.05, 0.1]$ is sufficient.

### 5.3 Mach 3 Step

We illustrate the algorithm described above by considering the Mach 3 flow in a wind tunnel with a forward facing step. This benchmark test has been proposed by Emery [5]. The geometry of the domain is shown in Fig. 3. The initial conditions are specified in terms of the primitive variables

$$(\rho, \mathbf{u}, p)^T(x, y, 0) = (1.4, (3.0, 0.0), 1.0)^T. \tag{28}$$

These initial conditions are also prescribed as inflow boundary conditions along the $\{x{=}0\}$ axis. The outflow boundary at $\{x{=}3\}$ is free. The slip condition $\mathbf{u}\cdot\mathbf{n} = 0$ is specified on the solid wall of the tunnel where $\mathbf{n}$ is the unit outward normal on $\partial\Omega$. This problem was popularized by Woodward and Colella's extensive study [24] of the performance of various numerical methods in the presence of strong shocks.

We show in Fig. 3 the density field at $t = 4$ on two different meshes with $\mathbb{P}_1$ Lagrange finite elements. The results shown in the left panels have been obtained on a mesh composed of 4813 $\mathbb{P}_1$ nodes and the results shown in the right panels have been obtained on a mesh composed of 893468 $\mathbb{P}_1$ nodes. These computations have been done with $c_{\max} = 0.25$, $c_E = 1$, $\mathcal{P} = 0.1$ and $\mathcal{P}_\rho = 0.1$. The tests have been run with CFL $= 0.5$. Our solutions agree, at least in the eye-ball norm, with other reference solutions that can be found in the literature. The contact discontinuity emerging from the three-shock interaction point is present in both simulations and is captured quite accurately. A Kelvin-Helmholtz instability develops along the contact discontinuity on the refined mesh.

As reported in [24] we have observed that the way the velocity boundary condition is implemented in the vicinity of the corner of the step somewhat influences the quality of the solution. We do not enforce any boundary condition at the node at the corner of the step in the computations shown in Fig. 3; enforcing the slip condition at this point implies $\mathbf{u} = 0$, which is too strong a constraint.

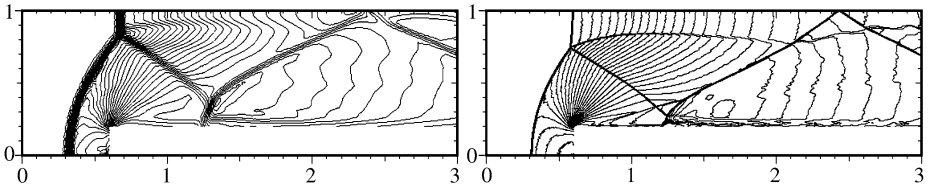


**Fig. 3** Mach 3 step, density, $t = 4$, density, $\mathbb{P}_1$ approximation. *Left*: $h = 0.25$, 4813 $\mathbb{P}_1$ nodes. *Right*: $h = 0.003$, 893468 $\mathbb{P}_1$ nodes

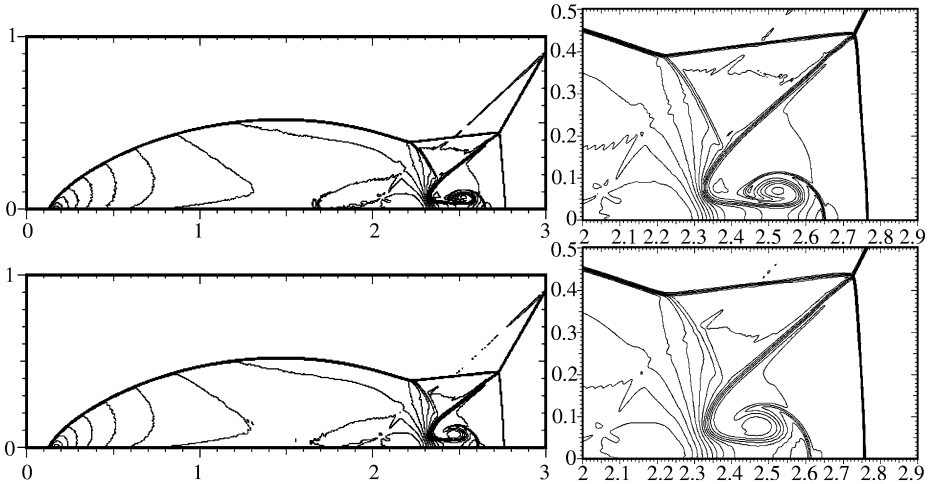


**Fig. 4** Double Mach reflection at $t = 0.2$, $M = 10$, density field, 453969 $\mathbb{P}_1$ nodes. *Left*: Global view. *Right*: Close up view in the region of three-shock interaction point. *Top*: $c_E = 0.25$. *Bottom*: $c_E = 1$

### 5.4 Double Mach Reflection

We now solve the so-called double Mach reflection problem at Mach 10. This problem, popularized by Woodward and Colella (see [24] for complete description), involves a Mach 10 shock in air ($\gamma = 1.4$) that impinges a wall with a 60 degree angle. The undisturbed air ahead of the shock has density 1.4 and pressure 1. The computational domain is $\Omega = (0, 4)\times(0, 1)$. The reflecting wall lies at the bottom of the domain and starts at $x = \frac{1}{6}$, i.e., free slip boundary condition is enforced on $\{x \geq \frac{1}{6}, y = 0\}$. The shock makes a 60 degree angle with the $x$-axis. Outflow boundary conditions are enforced at $\{0 \leq x < \frac{1}{6}, y = 0\}$ and $\{x = 4\}$. The values along the top boundary $\{y = 1\}$) are set to describe the motion of the initial Mach 10 shock. The flow is computed at time $t = 0.2$

The control parameters of the entropy viscosity are $c_{\max} = 0.25$, $c_E = 0.25$, $\mathcal{P} = 0.075$ and $\mathcal{P}_\rho = 0$. The tests have been run with CFL $= 0.5$

We show in Fig. 4 the solution computed with $\mathbb{P}_1$ Lagrange polynomials on a mesh composed of 453969 nodes. The left panel displays the density field in the region $0 \leq x \leq 3$. The right panel shows a close up view of the density in the region of the three-shock interaction point. To evaluate the influence of the control parameter $c_E$ we show in the bottom panel the density field computed with $c_E = 1$. The overall features are unchanged but using $c_E = 1$ slightly smeared the roll-up of the front jet and removed small oscillations.

### 5.5 A Riemann Problem with Fourier Approximation

We finish this series of tests by showing how the method performs with the Fourier approximation. The algorithm is the same as that described in Sect. 5.2, without using any stabilization term for the density, $\mathcal{P}_\rho = 0$, see [11].

The technique is validated by solving the benchmark problem number 12 from [22]. It is a two-dimensional Riemann problem set in $\mathbb{R}^2$. In the restricted computational domain

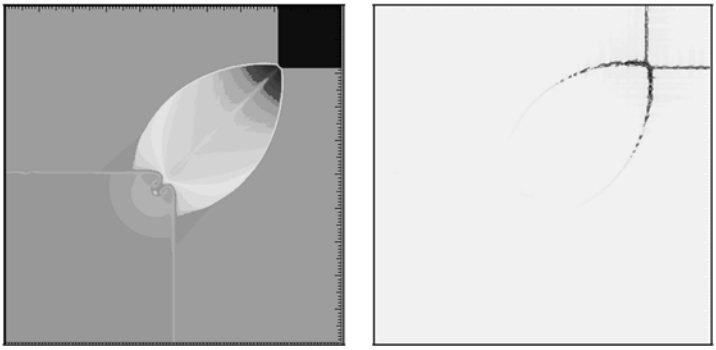

**Fig. 5** Riemann problem # 12, $t = 0.2$, 400×400 grid-points. *Left*: Density, $0.528 \leq \rho_h \leq 1.707$. *Right*: Viscosity, $0 \leq \mu_h < 3.410^{-3}$

$(0, 1)^2$ the initial set of data is defined as follows:

$$\begin{array}{llll} p = 1, & \rho = 4/5, & \mathbf{u} = (0, 0) & 0 < x < 1/2,\ 0 < y < 1/2, \\ p = 1, & \rho = 1, & \mathbf{u} = (3/\sqrt{17}, 0) & 0 < x < 1/2,\ 1/2 < y < 1, \\ p = 1, & \rho = 1, & \mathbf{u} = (0., 3/\sqrt{17}), & 1/2 < x < 1,\ 0 < y < 1/2, \\ p = 2/5, & \rho = 17/32, & \mathbf{u} = (0, 0), & 1/2 < x < 1,\ 0.5 < y < 1. \end{array} \tag{29}$$

Proceeding as in Sect. 4.3, the problem is first made periodic by extending the computational domain to $(0, 2)^2$, and the initial data are extended by symmetry about the axes $\{x = 1\}$ and $\{y = 1\}$. The solution is computed at time $t = 0.2$.

The time marching algorithm is the same as in Sect. 4.3. The nonlinear terms are dealiased. The control parameters for the entropy viscosity are $c_{\max} = \frac{1}{2}$, $c_E = 20$, and $\mathcal{P} = 1$.

We show in Fig. 5 results obtained with 400 Fourier modes in each direction, i.e., with 400 grid-points in $(0, 1)^2$. They compare well with those obtained with other more sophisticated shock capturing methods, see [22].

## 6 Conclusions

We have recalled basic mathematical properties of the three-dimensional incompressible Navier-Stokes equations and showed how they might relate to LES. Some fundamental questions regarding Fourier-based DNS have been raised. The notion of suitable solution lead us to introduce the new concept of entropy viscosity. The key idea consists of adding a numerical viscosity proportional to the default to equilibrium in the local energy equation. To evaluate this idea we have applied it to nonlinear conservation laws and showed that it is very efficient and very simple to implement.

Although the entropy/LES viscosity model (11) is mathematically justified and has been shown to behave well on nonlinear conservation laws including the compressible Euler equation, it cannot yet qualify as a validated LES model. To attain this status, it must be shown to perform well on simple turbulent flow settings and must be compared with other LES models. This program is currently being undertaken and the results will be reported in due time.

**Acknowledgements** This material is based upon work supported by the National Science Foundation grants DMS-07138229 and DMS-0811041 and partially supported by Award No. KUS-C1-016-04, made by King Abdullah University of Science and Technology (KAUST). This work was also supported by Lawrence Livermore National Security, LLC, under Task Order B575366 and Master Task Agreement B575363.

## References

1. Adams, N.A., Stolz, S.: A subgrid-scale deconvolution approach for shock capturing. J. Comput. Phys. **178**(2), 391–426 (2002)
2. Bardos, C., le Roux, A.Y., Nédélec, J.-C.: First order quasilinear equations with boundary conditions. Commun. Partial Differ. Equ. **4**(9), 1017–1034 (1979)
3. Bertoluzza, S.: The discrete commutator property of approximation spaces. C. R. Acad. Sci. Paris, Sér. I **329**(12), 1097–1102 (1999)
4. Caffarelli, L., Kohn, R., Nirenberg, L.: Partial regularity of suitable weak solutions of the Navier-Stokes equations. Commun. Pure Appl. Math. **35**(6), 771–831 (1982)
5. Emery, A.F.: An evaluation of several differencing methods for inviscid fluid flow problems. J. Comput. Phys. **2**, 306–331 (1968)
6. Gottlieb, S., Shu, C.-W., Tadmor, E.: Strong stability-preserving high-order time discretization methods. SIAM Rev. **43**(1), 89–112 (2001) (electronic)
7. Guermond, J.-L.: Finite-element-based Faedo-Galerkin weak solutions to the Navier-Stokes equations in the three-dimensional torus are suitable. J. Math. Pures Appl. **85**(3), 451–464 (2006)
8. Guermond, J.-L.: Faedo-Galerkin weak solutions of the Navier-Stokes equations with Dirichlet boundary conditions are suitable. J. Math. Pures Appl. **88**, 87–106 (2007)
9. Guermond, J.-L.: On the use of the notion of suitable weak solutions in CFD. Int. J. Numer. Methods Fluids **57**, 1153–1170 (2008)
10. Guermond, J.-L., Pasquetti, R.: Entropy-based nonlinear viscosity for Fourier approximations of conservation laws. C. R. Math. Acad. Sci. Paris **346**, 801–806 (2008)
11. Guermond, J.-L., Pasquetti, R.: Entropy viscosity method for high-order approximations of conservation laws. In: Ronquist, E. (ed.) ICOSAHOM09. Lecture Notes in Computational Science and Engineering, vol. 76, pp. 411–418. Springer, Berlin (2011)
12. Guermond, J.-L., Prudhomme, S.: On the construction of suitable solutions to the Navier-Stokes equations and questions regarding the definition of large eddy simulation. Physica D **207**, 64–78 (2005)
13. Hoffman, J., Johnson, C.: Computational Turbulent Incompressible Flow. Applied Mathematics: Body and Soul, vol. 4. Springer, Berlin (2007)
14. Hopf, E.: Über die Anfangswertaufgabe für die hydrodynamischen Grundgleichungen. Math. Nachr. **4**, 213–231 (1951)
15. Johnson, C., Szepessy, A.: On the convergence of a finite element method for a nonlinear hyperbolic conservation law. Math. Comput. **49**(180), 427–444 (1987)
16. Johnson, C., Szepessy, A., Hansbo, P.: On the convergence of shock-capturing streamline diffusion finite element methods for hyperbolic conservation laws. Math. Comput. **54**(189), 107–129 (1990)
17. Kružkov, S.N.: First order quasilinear equations with several independent variables. Mat. Sb. (N. S.) **81**(123), 228–255 (1970)
18. Kurganov, A., Petrova, G., Popov, B.: Adaptive semidiscrete central-upwind schemes for nonconvex hyperbolic conservation laws. SIAM J. Sci. Comput. **29**(6), 2381–2401 (2007) (electronic)
19. Leray, J.: Essai sur le mouvement d'un fluide visqueux emplissant l'espace. Acta Math. **63**, 193–248 (1934)
20. LeVeque, R.J.: Finite Volume Methods for Hyperbolic Problems. Cambridge Texts in Applied Mathematics. Cambridge University Press, Cambridge (2002)
21. Lin, F.: A new proof of the Caffarelli-Kohn-Nirenberg theorem. Commun. Pure Appl. Math. **51**(3), 241–257 (1998)
22. Liska, R., Wendroff, B.: Comparison of several difference schemes on 1D and 2D test problems for the Euler equations. SIAM J. Sci. Comput. **25**(3), 995–1017 (2003) (electronic)
23. Scheffer, V.: Hausdorff measure and the Navier-Stokes equations. Commun. Math. Phys. **55**(2), 97–112 (1977)
24. Woodward, P., Colella, P.: The numerical simulation of two-dimensional fluid flow with strong shocks. J. Comput. Phys. **54**(1), 115–173 (1984)